NORMAL BILIRUBINEMIA DOWNREGULATES THE POWER SPECTRAL DENSITY OF THE Θ AND Δ RHYTHM, INSTEAD UPREGULATES THE B RHYTHM AND SYMPATHO-VAGAL BALANCE IN ADULTS HUMANS

**Mykhaylo M. Korda[1], Anatoliy I. Gozhenko[2], Igor L. Kuchma[2],
Inna V. Korda[1], Oleksandr O. Popadynets'[2], Nataliya S. Badiuk[2],
Tetyana A. Korolyshyn[2,3], Walery Zukow[4], Igor L. Popovych[2,3]**

[1]IY Horbachevs'kyi National Medical University, Ternopil', Ukraine
kordai@tdmu.edu.ua; kordamm@yahoo.com
**[2]Ukrainian Scientific Research Institute of Medicine for Transport Ministry of Health,
Odesa, Ukraine prof.gozhenko@gmail.com; badiuk_ns@ukr.net; igorkuchma@ukr.net**
[3]OO Bohomolets' Institute of Physiology of NAS, Kyïv, Ukraine
i.popovych@biph.kiev.ua; korolushyn@gmail.com
[4]Nicolaus Copernicus University, Torun, Poland w.zukow@wp.pl

Abstract

Background. *Neonatal hyperbilirubinemia* has been known to damage neural function. Our goal is to determine whether the neurotropic activity of *normal* bilirubinemia in *adults* is evident. **Methods**. The object of observation were 77 volunteers: 30 women and 47 men aged 49 ± 13 ($26 \div 76$) years without clinical diagnosis. Testing was performed twice with an interval of $4 \div 10$ days. We determined the plasma levels of the direct and free bilirubin, recorded EEG and HRV followed by analysis of correlations between parameters. **Results**. Significant downregulating effect of bilirubinemia was found on power spectrum density (PSD) theta and delta rhythm. In contrast, bilirubinemia has an upregulating effect on PSD beta rhythm and sympatho-vagal balance. The canonical correlation between direct & free bilirubin levels, on the one hand, and EEG & HRV parameters, on the other hand, is very strong: $R=0,808$; $R^2=0,654$; $\chi^2_{(80)}=191$; $p<10^{-6}$ (n=154). A similar canonical correlation was found between individual changes in parameters: $R=0,753$; $R^2=0,568$; $\chi^2_{(48)}=83$; $p=0,001$ (n=74). **Conclusion**. Even normal bilirubinemia has an downregulating effect on mainly theta and delta rhythm-generating nuclei and vagal tone, while upregulating effects on sympathetic tone and beta rhythm-generating nuclei.
Keywords: bilirubinemia, EEG, HRV, relationships, adults humans.

INTRODUCTION

Neonatal hyperbilirubinemia has been known to damage neural function and morphology [Shapiro SM et Conlee JW, 1991]. Accumulation of bilirubin in the central nervous system results in neurotoxicity in areas such as the ventral cochlear nucleus, vestibular nuclei, cerebellum, and **hippocampus** [Watchko JF, 2006]. Bilirubin-induced neurotoxicity is widely accepted as a leading cause of hearing loss, balance, motor control, and cognition deficits in children with severe clinical hyperbilirubinemia, and is often aggravated by confounding factors such as prematurity, infection, sepsis, hypoxia, ischemia, and acidosis [Dennery PA et al, 2001; Watchko JF et Tiribelli C, 2013], all of which may increase the permeability of blood-brain barrier to bilirubin.

Chang FY et al [2009] find that exposure of **hippocampal** slice cultures to clinically relevant concentrations of unconjugated bilirubin (UCB) for 24 or 48 h results in an impairment of CA1 long-term potentiation (LTP) and long-term depression (LTD) induction in a time- and concentration-dependent manner as well as significant decrease in the levels of subunits of *N*-methyl-D-aspartate (NMDA) receptors. Pretreatment of the hippocampal slice cultures with NMDA receptor antagonist or calpain inhibitors effectively prevented the UCB-induced impairment of LTP and LTD. These results indicate that the proteolytic cleavage of NMDA receptor subunits by calpain may play a critical role in mediating the UCB-induced **impairment** of long-term synaptic plasticity in the **hippocampus**.

Dani C et al [2019] hypothesized that oxidative stress may be a common mechanism that link hyperbilirubinemia and hypoxic-ischemic encephalopathy (HIE). The effects of UCB were tested on rat organotypic **hippocampal** slices subjected to 30 min oxygen-glucose deprivation (OGD), used as *in vitro* model of HIE. The experiments were performed on mature (14 days in culture) and immature (7 days in culture) slices, to mimic the brains of term and preterm infants, respectively. Mature and immature slices were exposed to UCB, human serum albumin (HSA), pioglitazone, and/or allopurinol for 24 h, immediately after 30 min OGD. Neuronal injury was assessed using propidium iodide fluorescence. In mature slices, authors found that the neurotoxicity, as well as oxidative stress, were enhanced by UCB. HSA significantly prevented UCB-increased neurotoxicity, but had a slight reduction on ROS production. Allopurinol, but not pioglitazone, significantly reduced UCB-increased neurotoxicity induced by OGD. In immature slices exposed to OGD, no increase of neuronal death was observed, whereas oxidative stress was detected after UCB exposure. HSA, pioglitazone and allopurinol have no protective effects on both OGD-induced neuronal death and on UCB-induced oxidative stress. For this reason, UCB, pioglitazone and allopurinol was also tested on ischemic preconditioning protocol. The authors found that UCB abolished the neuroprotection induced by preconditioning and increased oxidative stress. These effects were restored by allopurinol but not pioglitazone. The authors came to the conclusions that UCB characterized a different path of neuronal damage and oxidative stress in mature and immature **hippocampal** slice model of HIE. Management of hyperbilirubinemia in a complex pathological condition, such as HIE and hyperbilirubinemia, should be very careful. Allopurinol could deserve attention as a novel pharmacological intervention for hyperbilirubinemia and HIE.

The aim of next Dani C et al [2021] study was to assess the effect on bilirubin neurotoxicity of the maturity or immaturity of exposed cells, the influence of different UCB and HSA concentrations, and time of UCB exposure. **Hippocampal** slices were exposed for 48 h to different UCB and HSA concentrations after mature or immature culture. Immature slices were also exposed to UCB and HSA for 72 h. The different effects of exposure time to UCB on neurons and astrocytes were evaluated. The authors found that 48 h of UCB exposure was neurotoxic for mature **hippocampal** slices while 72 h of exposure was neurotoxic for immature slices. 48 h UCB exposure was toxic for astrocytes but not for neurons, while 72-h

exposure was toxic for both astrocytes and neurons. HSA prevented UCB toxicity when the UCB/HSA molar ratio was ≤1 in both mature and immature slices. Thus, the authors confirmed UCB neurotoxicity in mature and immature rat **hippocampal** slices, although immature ones were more resistant; HSA was effective in preventing UCB neurotoxicity in both mature and immature rat hippocampal slices.

Bilirubin can increase neuronal excitability and spontaneous firings in developing neurons, possibly allowing Ca^{2+} influx via VGCCs as well as intracellular Ca^{2+} release from internal stores [Liang M et al, 2017; Han G-Y et al, 2015]. The elevated $[Ca^{2+}]i$ in turn increases CaMKII-dependent phosphorylation of acid-sensing ion channels (ASICs) and potentiates the amplitude of IASICs [Chai S et al, 2007; Allen NJ et Attwell D, 2002].

Lai K et al [2020] demonstrated in mouse **neonatal** neurons that **hyperbilirubinemia** exhibited **marginal neurotoxicity** on its own, but potentiated the currents mediated by ASIC1a channels in an acidic environment via Ca^{2+}-dependent intracellular signaling, and jointly boosted neuronal excitability, Ca^{2+} overload, and cell death. They found that all the brain slices from the acidosis and acidosis+hyperbilirubinemia groups were stained blue, especially in the **hippocampus**, brainstem, and cerebellum with minimal staining of the cortex. The authors postulate that bilirubin itself has limited toxicity but may exacerbate acidosis-dependent neuronal damage.

Our goal is to determine whether the **neurotropic** activity of **normal bilirubinemia** in **adults** is evident.

MATERIAL AND METHODS

The object of observation were 77 volunteers: 30 women and 47 men aged 49±13 (26 ÷ 76) years without clinical diagnosis. Testing was performed twice with an interval of 4 ÷ 10 days.

We determined the plasma levels of the direct (conjugated) and free (unconjugated) bilirubin (by diazoreaction using the Jedrashik-Kleghorn-Grof method). The analyzes were carried out according to the instructions described in the manual [Goryachkovskiy AM, 1998]. The analyzer "Reflotron" (Boehringer Mannheim, BRD) were used with appropriate sets.

To assess the parameters of heart rate variability (HRV) recorded (TA Korolyshyn) during 7 min electrocardiogram in II lead (software and hardware complex "CardioLab+HRV", KhAI-MEDICA, Kharkiv). For further analysis the following parameters HRV were selected [Heart Rate Variability, 1996; Berntson GG et al, 1997; Baevskiy RM & Ivanov GG, 2001; Shaffer F & Ginsberg JP, 2017]. Temporal parameters (Time Domain Methods): the standard deviation of all NN intervals (SDNN), the square root of the mean of the sum of the squares of differences between adjacent NN intervals (RMSSD), the percent of interval differences of successive NN intervals greater than 50 msec (pNN_{50}). Spectral parameters (Frequency Domain Methods): power spectrum (PS) bands of HRV - high-frequency (HF, range 0,4÷0,15 Hz), low-frequency (LF, range 0,15÷0,04 Hz), very low-frequency (VLF, range 0,04÷0,015 Hz) and ultralow-frequency (ULF, range 0,015÷0,003 Hz). Calculated classical indexes LF/HF, (VLF+LF)/HF and LFnu=100%•LF/(LF+HF).

Simultaneosly EEG recorded (TA Korolyshyn) a hardware-software complex "NeuroCom Standard" (KhAI MEDICA, Kharkiv) monopolar in 16 loci (Fp1, Fp2, F3, F4, F7, F8, C3, C4, T3, T4, P3, P4, T5, T6, O1, O2) by 10-20 international system, with the reference electrodes A and Ref tassels on the ears. The duration of the epoch was 25 sec. Among the options considered the average EEG amplitude (μV), average frequency (Hz), frequency deviation (Hz) as well as absolute ($μV^2$/Hz) and relative (%) power spectrum density (PSD) of basic rhythms: β (35÷13 Hz), α (13÷8 Hz), θ (8÷4 Hz) and δ (4÷0,5 Hz) in all loci, according to the instructions of the device.

We calculated also for each locus EEG and HRV Shannon's CE entropy (h) of normalized PSD using Popovych's IL formulas [Kul'chyns'kyi AB et al, 2017; Popadynets' OO et al, 2020; Gozhenko AI et al, 2021]:

$hEEG = - [PSD\alpha \cdot \log_2 PSD\alpha + PSD\beta \cdot \log_2 PSD\beta + PSD\theta \cdot \log_2 PSD\theta + PSD\delta \cdot \log_2 PSD\delta]/\log_2 4$

$hHRV = -[PSHF \cdot \log_2 PSHF + PSLF \cdot \log_2 PSLF + PSVLF \cdot \log_2 PSVLF + PSULF \cdot \log_2 PSULF]/\log_2 4$

Results processed by using the software package "Statistica 64".

RESULTS AND DISCUSSION

First of all, it was stated that the levels of both bilirubin fractions exceeded the norm in only two samples out of 154 (Fig. 1).
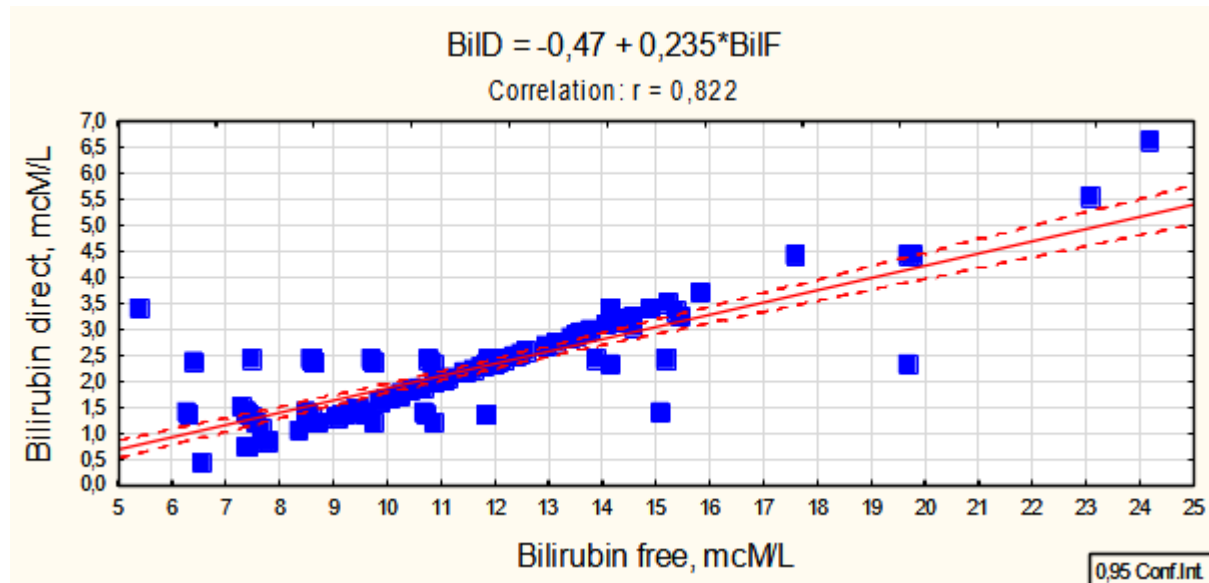
Fig. 1. Scatterplot of correlation between Bilirubin free (X-line) and direct (Y-line) plasma levels

In the first stage, correlations between bilirubin levels and EEG and HRV parameters were screened.

According to the formula: $|r| = \{\exp[2t/(n-1,5)^{0,5}]-1\}/\{\exp[2t/(n-1,5)^{0,5}]+1\}$
for a sample of n=154 critical value $|r|$ at p<0,05 (t>2,00) is 0,16, at p<0,01 (t>2,66) is 0,21, at p<0,001 (t>3,46) is 0,27.

The correlation with the relative PSD of theta rhythm in the T5 locus was the closest (Fig. 2). Interestingly, the downregulating effect of Direct Bilirubin outweighs that of Free Bilirubin (-0,428 vs -0,276). Correlation screening revealed that with 29 EEG parameters the **negative** correlation is stronger for direct bilirubin, with 14 EEG parameters and relative power of HF band HRV the negative correlation coefficients are almost the same as the **positive** ones with relative powers of LF and VLF bands as well as PSD T4-β (Fig. 3).
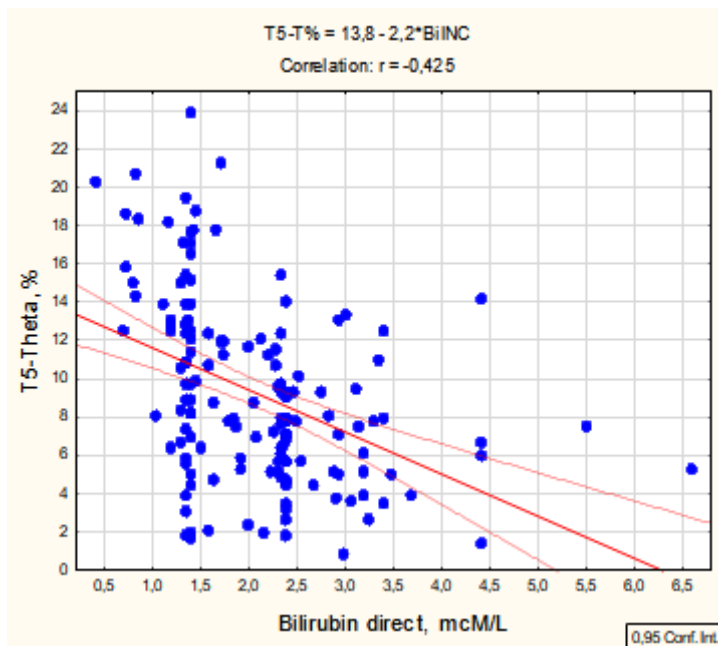
Fig. 2. Scatterplot of correlation between Bilirubin direct (X-line) and PSD of theta rhythm in locus T5 (Y-line)
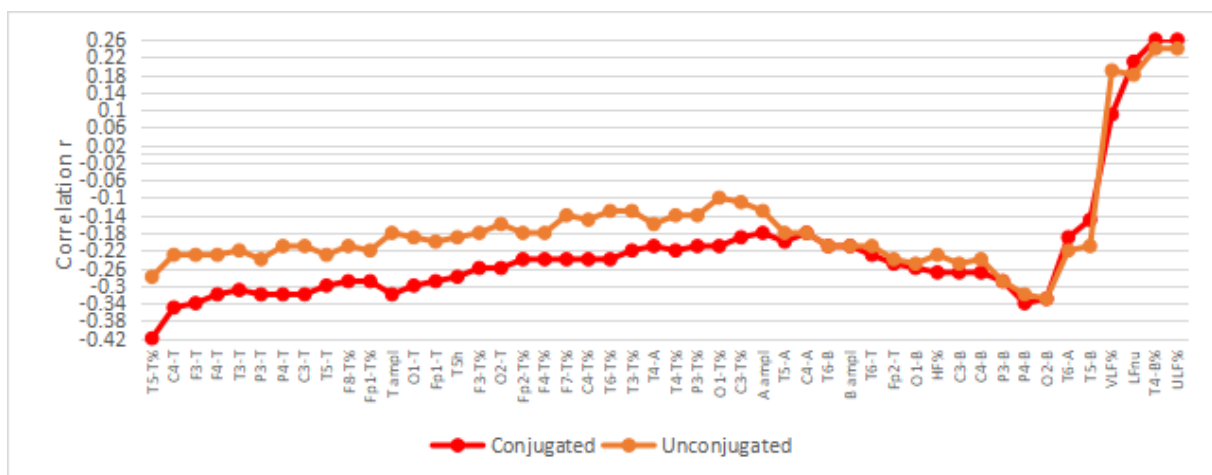
Fig. 3. Profiles of significant correlation coefficients of bilirubinemia with EEG and HRV parameters

In the next step of the analysis, a regression model was constructed by stepwise exclusion until the maximum level of adjusted R^2 was reached. As a result, it turned out that regression models included parameters with an low correlation coefficient, while some parameters with a significant correlation were outside the model. Now let's analyze each regression model.

From the first regression model it follows that Direct Bilirubin **downregulates** the PSD of **theta** rhythm in 5 left and 2 right loci, while **beta** rhythm downregulation occurs in 3 left and 3 right loci. In contrast, at the T4 locus, bilirubinemia **upregulates** PSD beta rhythm. Interestingly, with PSD beta rhythm in the contralateral locus (T3) the correlation is insignificant (r=0,15), as in the neighboring locus T5 (r= -0,15), while with PSD in the ipsilateral neighboring locus T6 it is significantly **negative** (r= -0,23). The **opposite** sign of the relationship was found with the relative spectral power of HF and ULF bands of HRV

458

(Table 1). Judging by the coefficient of determination, the neuromodulatory effect of plasma levels of conjugated bilirubin is 64% (Fig. 4).

Table 1. Regression Summary for Bilirubin direct
R=0,797; R^2=0,636; Adjusted R^2=0,578; $F_{(21)}$=11,0; $p<10^{-4}$

N=154		Beta	St. Err. of Beta	B	St. Err. of B	$t_{(132)}$	p-level
Variables	r		Intercpt	2,810	0,364	7,71	10^{-6}
T5-θ PSD, %	-0,42	-0,709	0,104	-0,137	0,020	-6,82	10^{-6}
F3-θ PSD, μV²/Hz	-0,34	-0,234	0,131	-0,0039	0,0022	-1,78	0,077
P4-β PSD, μV²/Hz	-0,34	-0,666	0,163	-0,0100	0,0024	-4,09	10^{-4}
O2-β PSD, μV²/Hz	-0,33	0,186	0,106	0,0030	0,0017	1,76	0,081
C3-θ PSD, μV²/Hz	-0,32	0,347	0,145	0,0062	0,0026	2,40	0,018
T3-θ PSD, μV²/Hz	-0,31	-0,285	0,111	-0,0059	0,0023	-2,56	0,011
T5-θ PSD, μV²/Hz	-0,30	0,415	0,122	0,0089	0,0026	3,41	0,001
P3-β PSD, μV²/Hz	-0,29	-0,248	0,176	-0,0031	0,0022	-1,41	0,161
Entropy T5	-0,28	0,149	0,093	0,770	0,481	1,60	0,112
HF HRV PS, %	-0,27	-0,267	0,060	-0,025	0,006	-4,45	10^{-4}
C3-β PSD, μV²/Hz	-0,27	0,210	0,151	0,0027	0,0019	1,39	0,167
O1-β PSD, μV²/Hz	-0,25	-0,170	0,109	-0,0023	0,0015	-1,56	0,122
Fp2-θ PSD, μV²/Hz	-0,25	0,151	0,094	0,0036	0,0023	1,61	0,110
T4-θ PSD, %	-0,22	0,146	0,078	0,027	0,015	1,86	0,065
P3-θ PSD, %	-0,21	-0,154	0,080	-0,030	0,016	-1,92	0,057
T6-β PSD, μV²/Hz	-0,21	-0,343	0,077	-0,0046	0,0010	-4,47	10^{-4}
Amplitude β, μV	-0,21	0,186	0,108	0,045	0,026	1,73	0,086
Amplitude α, μV	-0,18	-0,289	0,116	-0,024	0,010	-2,49	0,014
C4-α PSD, μV²/Hz	-0,18	0,296	0,136	0,0015	0,0007	2,17	0,032
T4-β PSD, %	0,26	0,439	0,069	0,025	0,004	6,38	10^{-6}
ULF HRV PS, %	0,26	0,172	0,059	0,023	0,008	2,94	0,004
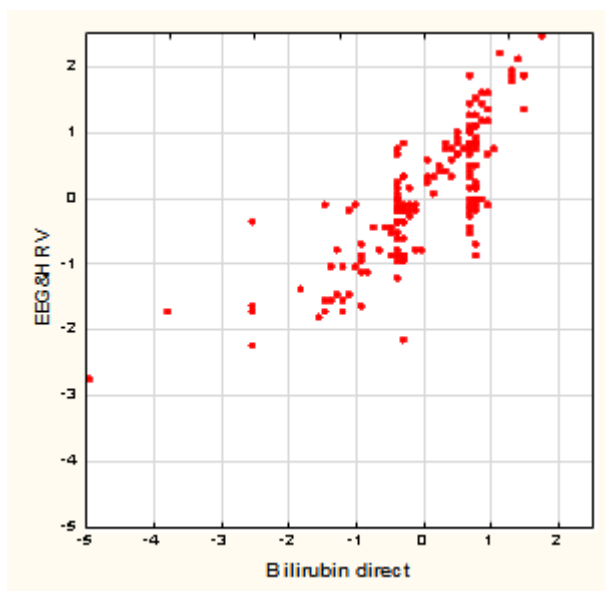
R=0,797; R^2=0,636; $\chi^2_{(21)}$=143; $p<10^{-5}$; Λ Prime=0,364

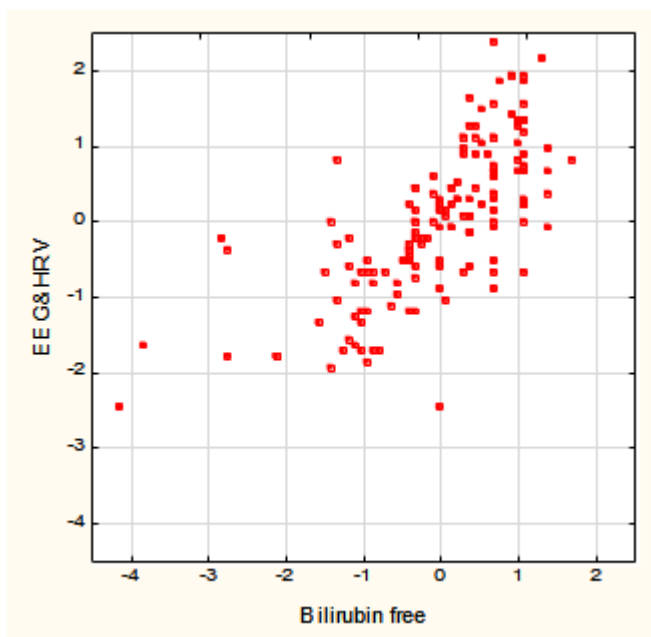**Fig. 4. Scatterplot of canonical correlation between Bilirubin direct (X-line) and EEG&HRV parameters (Y-line)**

Despite significant links to the PSD of theta rhythm, the loci F4 (r= -0,32), Fp1 (r= -0,29), F8 (r= -0,29) and F7 (r= -0,24), was out of the model, apparently due to duplication and/or redundancy of information.

Unconjugated bilirubin is expected to have a lower effect on EEG and HRV parameters, determining them by only 51% (Table 2 and Fig. 5).

Table 2. Regression Summary for Bilirubin free
R=0,712; R^2=0,507; Adjusted R^2=0,441; $F_{(18)}$=7,7; $p<10^{-5}$

N=154		Beta	St. Err. of Beta	B	St. Err. of B	$t_{(135)}$	p-level
Variables	r		Intercpt	9,446	1,696	5,57	10^{-6}
P4-β PSD, µV²/Hz	**-0,32**	-0,614	0,138	-0,0323	0,0073	-4,46	10^{-4}
T5-θ PSD, %	**-0,28**	-0,592	0,110	-0,400	0,075	-5,36	10^{-6}
Fp2-θ PSD, µV²/Hz	**-0,24**	-0,175	0,123	-0,0148	0,0104	-1,42	0,158
F3-θ PSD, µV²/Hz	**-0,23**	-0,239	0,155	-0,0138	0,0089	-1,55	0,125
C4-θ PSD, µV²/Hz	**-0,23**	0,264	0,176	0,0146	0,0097	1,50	0,137
HF HRV PS, %	**-0,23**	-0,211	0,071	-0,069	0,023	-2,98	0,003
T6-α PSD, µV²/Hz	**-0,22**	-0,107	0,102	-0,0019	0,0018	-1,05	0,297
T3-θ PSD, µV²/Hz	**-0,22**	-0,216	0,109	-0,0155	0,0079	-1,97	0,050
C3-θ PSD, µV²/Hz	**-0,21**	0,410	0,173	0,0257	0,0108	2,37	0,019
Amplitude β, µV	**-0,21**	0,232	0,122	0,195	0,102	1,91	0,058
T5-β PSD, µV²/Hz	**-0,21**	-0,152	0,092	-0,0064	0,0039	-1,65	0,100
T6-β PSD, µV²/Hz	**-0,21**	-0,316	0,087	-0,0148	0,0041	-3,63	10^{-3}
T6-θ PSD, µV²/Hz	**-0,21**	0,123	0,114	0,0087	0,0081	1,08	0,281
Entropy T5	**-0,19**	0,150	0,101	2,709	1,825	1,48	0,140
Amplitude θ, µV	**-0,18**	0,335	0,126	0,257	0,096	2,66	0,009
T4-β PSD, %	**0,24**	0,407	0,075	0,081	0,015	5,40	10^{-6}
ULF HRV PS, %	**0,24**	0,103	0,068	0,049	0,032	1,51	0,133
(VLF+ULF) PS, %	**0,19**	0,098	0,073	0,019	0,014	1,34	0,181

R=0,712; R^2=0,507; $\chi^2_{(18)}$=101; $p<10^{-5}$; Λ Prime=0,493

Fig. 5. Scatterplot of canonical correlation between Bilirubin free (X-line) and EEG&HRV parameters (Y-line)

Canonical correlation analysis shows that the combined neuromodulatory effect of both bilirubin fractions outweighs their partial effects (Fig. 6).

Applied pseudo-staining clearly shows (Table 3) that bilirubin **downregulates** mainly nerve structures that generate **theta** rhythm, and to a lesser extent, **beta** and **alpha** rhythm-generating nuclei, as well as **entropy** in locus T5 and **vagal** tone. Instead, the beta-generating nuclei projected at the T4 locus, as well as the HRV marker of sympathetic tone are **upregulated**.

This is where it is appropriate to talk about the VLF and ULF bands, given their ambiguous interpretation. Let's take advantage of the latest wonderful review Shaffer F & Ginsberg JP [2017]. We quote. "There is uncertainty regarding the physiological mechanisms responsible for activity within the VLF (0,04÷0,0033 Hz) band. The heart's intrinsic nervous system appears to contribute to the VLF rhythm and the sympathetic nervous system influences the amplitude and frequency of its oscillations. Very-low-frequency power may also be generated by physical activity, thermoregulatory, renin–angiotensin, and endothelial influences on the heart. Vagal activity may contribute to VLF power since parasympathetic blockade almost completely abolishes it. In contrast, sympathetic blockade does not affect VLF power and VLF activity is seen in tetraplegics, whose sympathetic nervous system innervation of the heart and lungs is disrupted. The VLF rhythm appears to be generated by the stimulation of afferent sensory neurons in the heart. This, in turn, activates various levels of the feedback and feed-forward loops in the heart's intrinsic cardiac nervous system, as well as between the heart, the extrinsic cardiac ganglia, and spinal column. This experimental evidence suggests that the heart intrinsically generates the VLF rhythm and efferent sympathetic nervous system activity due to physical activity and stress responses modulates its amplitude and frequency".

Because in our device ULF band (range 0,015÷0,003 Hz) is integrated into the lower zone of VLF band, what has been said about the latter also applies to the former. By the way, the relative PS of these bands during the analysis were combined into an option (VLF+ULF).

Table 3. Factor structure of canonical Roots representing the Bilirubinemia and EEG&HRV parameters (n=154)

Left side	R1
Bilirubin direct	-1,000
Bilirubin free	-0,819
Right side	**R1**
T5-θ PSD, %	0,526
T5-θ PSD, µV²/Hz	0,375
C4-θ PSD, µV²/Hz	0,432
F3-θ PSD, µV²/Hz	0,423
P4-β PSD, µV²/Hz	0,419
O2-β PSD, µV²/Hz	0,413
F4-θ PSD, µV²/Hz	0,402
C3-θ PSD, µV²/Hz	0,393
Amplitude θ, µV	0,393
P4-θ PSD, µV²/Hz	0,391
P3-θ PSD, µV²/Hz	0,390
T3-θ PSD, µV²/Hz	0,380
O1-θ PSD, µV²/Hz	0,371
F8-θ PSD, %	0,364
Fp1-θ PSD, %	0,364
P3-β PSD, µV²/Hz	0,356
Entropy T5	0,344
C4-β PSD, µV²/Hz	0,339

C3-β PSD, µV²/Hz	0,328
O2-θ PSD, µV²/Hz	0,325
Fp2-θ PSD, µV²/Hz	0,308
C4-θ PSD, %	0,303
O1-β PSD, µV²/Hz	0,303
T6-θ PSD, %	0,297
T6-θ PSD, µV²/Hz	0,288
T4-θ PSD, %	0,272
P3-θ PSD, %	0,264
T4-α PSD, µV²/Hz	0,264
Amplitude β, µV	0,260
T6-β PSD, µV²/Hz	0,254
T5-α PSD, µV²/Hz	0,244
T6-α PSD, µV²/Hz	0,232
C4-α PSD, µV²/Hz	0,223
Amplitude α, µV	0,219
T5-β PSD, µV²/Hz	0,181
HF HRV PS, %	0,330
T4-β PSD, %	-0,324
ULF HRV PS, %	-0,320
LF/(LF+HF), %	-0,263
(VLF+ULF) PS, %	-0,105
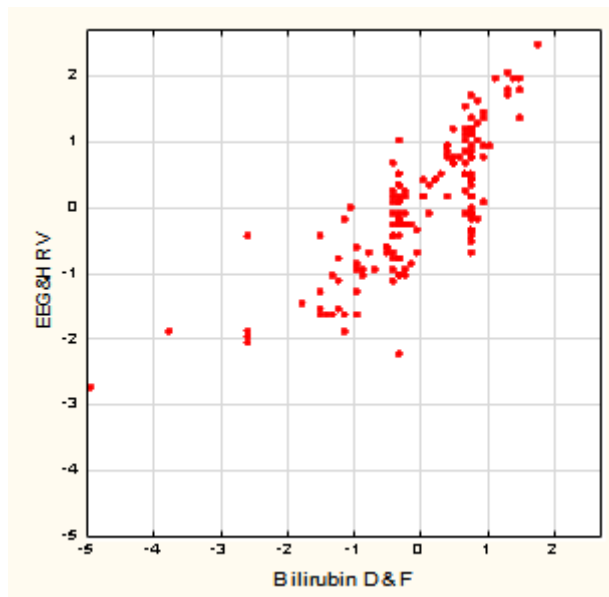
$R=0,808$; $R^2=0,654$; $\chi^2_{(80)}=191$; $p<10^{-6}$; Λ Prime=0,236

Fig. 6. Scatterplot of canonical correlation between Bilirubin levels (X-line) and EEG&HRV parameters (Y-line)

HRV parameters, in turn, are subject to opposite regulatory influences of theta rhythm-generating nuclei (Table 4 and Fig. 7).

Table 4. Factor structure of canonical Roots representing the EEG and HRV parameters

Left side	R
C4-θ PSD, μV²/Hz	0,354
C3-θ PSD, μV²/Hz	0,249
T5-θ PSD, μV²/Hz	-0,299
P3-θ PSD, %	-0,241
Right side	R
HF HRV PS, %	0,981
LF/(LF+HF), %	-0,842
(VLF+ULF) PS, %	-0,531
ULF HRV PS, %	-0,115
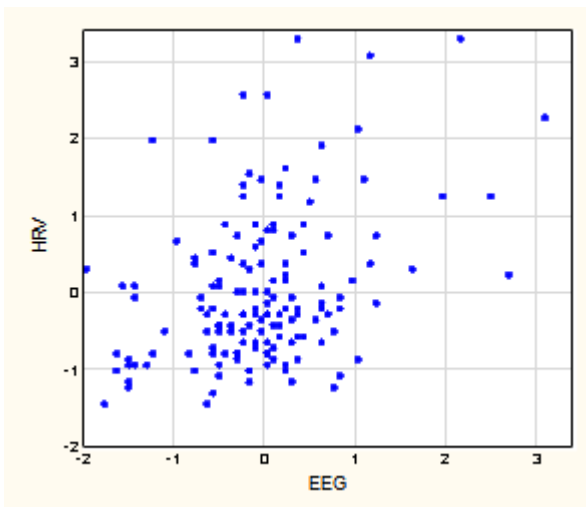
R=0,386; R^2=0,149; $\chi^2_{(30)}$=50; p=0,013; Λ Prime=0,712

Fig. 7. Scatterplot of canonical correlation between EEGs (X-line) and HRVs (Y-line) parameters

Next, we analyzed the correlation between **individual changes** (influenced by various factors not related to this topic) in bilirubinemia and electrical activity of the brain. This approach, in our opinion, is more informative.

Here are examples of opposite regulatory effects of direct bilirubin on PSD (Figs. 8 and 9).

Fig. 8. Scatterplot of correlation between changes in Bilirubin direct (X-line) and PSD of theta rhythm in locus T5 (Y-line)
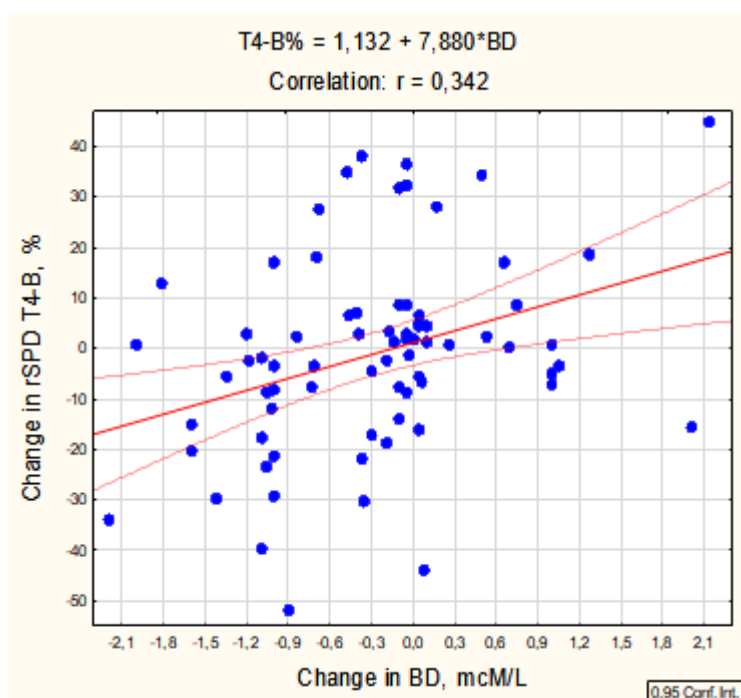
Fig. 9. Scatterplot of correlation between changes in Bilirubin direct (X-line) and PSD of beta rhythm in locus T4 (Y-line)

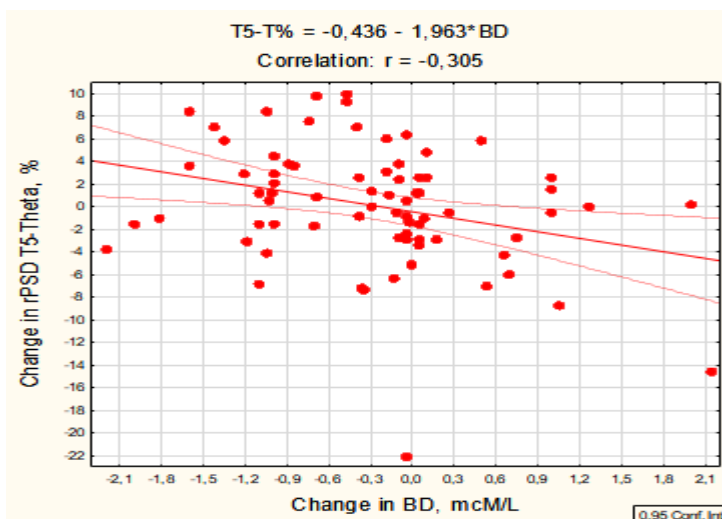Despite a twofold decrease in the sample size, the strength of the canonical correlation, especially for conjugated bilirubin, did not decrease. However, in regression models **delta** rhythm parameters appeared and the number of loci subject to upregulation increased (Table 5 and Fig. 8).

It was found that changes in bilirubinemia are accompanied by **opposite** changes in the amplitude of **theta** rhythm and its relative and/or absolute SPD in 10 loci, the amplitude of **delta** rhythm and its relative and/or absolute SPD in 5 loci, as well as PSD **T6-β**. Instead, was found **unidirectionally** with bilirubinemia changes in PSD **beta** rhythm in 5 loci, **alpha** rhythm in three left loci and **entropy** in locus T3, as well as **HRV-markers** of sympatho-vagal balance, autonomous regulation centralization and sympathetic tone.

Table 5. Factor structure of canonical Roots representing the changes in the Bilirubinemia and EEG&HRV parameters (n=74)

Left side	R1
Bilirubin direct	**-0,988**
Bilirubin free	**-0,808**
Right side	**R1**
Fp2-θ PSD, %	**0,538**
Fp2-θ PSD, μV²/Hz	**0,392**
F3-θ PSD, μV²/Hz	**0,469**
F3-θ PSD, %	**0,324**
Amplitude θ, μV	**0,443**
T6-δ PSD, μV²/Hz	**0,417**
Fp1-θ PSD, μV²/Hz	**0,407**
Fp1-θ PSD, %	**0,345**
T5-θ PSD, %	**0,403**
F8-θ PSD, μV²/Hz	**0,390**

F8-θ PSD, %	**0,366**
P3-θ PSD, %	**0,357**
P3-θ PSD, µV²/Hz	**0,320**
C4-θ PSD, µV²/Hz	**0,356**
T4-δ PSD, %	**0,354**
T6-θ PSD, µV²/Hz	**0,338**
Amplitude δ, µV	**0,332**
C3-θ PSD, µV²/Hz	**0,331**
F4-θ PSD, µV²/Hz	**0,309**
P3-δ PSD, µV²/Hz	**0,287**
P3-δ PSD, %	**0,250**
F7-δ PSD, µV²/Hz	**0,248**
C3-δ PSD, µV²/Hz	**0,235**
C3-δ PSD, %	**0,216**
T6-β PSD, µV²/Hz	**0,286**
T4-β PSD, %	**-0,427**
F3-β PSD, %	**-0,363**
F4-β PSD, %	**-0,332**
Fp2-β PSD, %	**-0,324**
C3-β PSD, %	**-0,183**
P3-α PSD, %	**-0,320**
T3-α PSD, %	**-0,296**
C3-α PSD, %	**-0,234**
Entropy T3	**-0,293**
LF/HF	**-0,247**
(VLF+LF)/HF	**-0,217**
LF HRV PS, ms²	**-0,194**
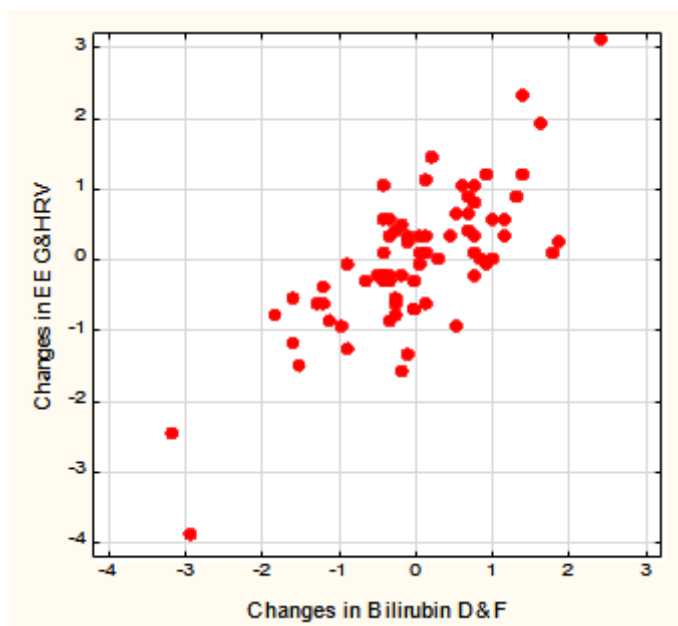
R=0,753; R^2=0,568; $\chi^2_{(48)}$=83; p=0,0014; Λ Prime=0,249

Fig. 10. Scatterplot of canonical correlation between changes in Bilirubin levels (X-line) and EEG&HRV parameters (Y-line)

DISCUSSION

First of all, we have shown that even **normal bilirubinemia** shows **neuromodulatory** activity in **adults**, not just **hyperbilirubinemia in newborns**. Bilirubin, more direct, less free, **downregulates** the electrical activity of nuclei that generate **theta** rhythm. It is well known

that the main generator of **theta** rhythm is the **hippocampus** [Buzsaki G, 2002] - a favorite object of experimental studies of **neurotoxicity of bilirubin**.

It is believed that the hippocampus is projected at the C3 and C4 loci [Romodanov AP, 1993]. Based on this position, we found that direct (R= -0,988) and free (R= -0,808) bilirubin **downregulates** the activity of neurons in both the right (R=0,356) and left (R=0,331) hippocampus, which generate **theta** rhythm, as well as neurons of the left hippocampus, which generate **delta** rhythm (R=0,235). However, bilirubin **upregulates** neurons in the left hippocampus, which generate **alpha** (R= -0,234) and **beta** (R= -0,183) rhythms.

According to the concept of "central autonomic network (CAN)" [Benarroch EE, 1993; Palma JA & Benarroch EE, 2014; Thayer JF & Lane RD, 2009] it include following cortical, subcortical, and medullary structures: the anterior cingulate, insular, orbitofrontal, and ventromedial cortices; the central nucleus of the amygdala; the paraventricular and related nuclei of the hypothalamus; the periaqueductal gray matter; the nucleus of the solitary tract; the nucleus ambiguous; the ventrolateral medulla; the ventromedial medulla and the medullary tegmental field. The primary output of the CAN is mediated through the preganglionic sympathetic and parasympathetic neurons, which exert control over the heart via the stellate ganglia and the vagus nerve, respectively. The interplay of sympathetic and parasympathetic influences on sinoatrial node pacemaker activity generates the complex variability that characterizes the healthy heart rate rhythm, which is called HRV. A fundamental principle of the neural control of the heart is its hierarchical organization, with cortical structures providing inhibitory control over limbic and brainstem sympathoexcitatory, cardioacceleratory circuits. The prefrontal, cingulate, and insula cortices form an interconnected network with bi-directional communication with the amygdala. The amygdala is under tonic inhibitory control via prefrontal vagal pathways to intercalated cells in the amygdala. The activation of the central nucleus of the amygdala (CeA) inhibits the nucleus of the solitary tract (NTS) which in turn inhibits inhibitory caudal ventrolateral medullary (CVLM) inputs to the rostral ventrolateral medullary (RVLM) sympathoexcitatory neurons, and simultaneously inhibits vagal motor neurons in the nucleus ambiguus (NA) and the dorsal vagal motor nucleus (DVN). In addition, the CeA can directly activate the sympathoexcitatory neurons in the RVLM. Indeed, disruption of prefrontal activity leads to disinhibition of sympathoexcitatory circuits, with a resultant increase in heart rate and decrease in vagally-mediated HRV [Verberne AJ et al, 1996; 1997; Gianaros PJ, 2008; Thayer JF & Lane RD, 2009; Sakaki M et al, 2016]. Conversely, let's add from ourselves, activation of prefrontal cortex leads to increase in vagal tone.

Iseger TA et al [2017] applied trains of transcranial magnetic stimulation (rTMS) over 7 cortical regions aiming to identify which regions would affect heart rate. They found that F3 and F4 expressed the largest heart rate deceleration, in line with studies suggesting these are the best sites to target the dorsolateral prefrontal cortex (DLPFC). On the individual level, 20-40% subjects expressed the largest heart rate deceleration at FC3 or FC4, indicating individual differences as to the 'optimal site for stimulation'. Interestingly, stimulation of the C3, C4 and Pz loci showed opposite effects. But Remue J et al [2016] found that after real HF-rTMS over the left DLPFC the physiological stress response was diminished, as indicated by a significant increase in HRV. No effects were found in the sham or right side stimulation condition. This is consistent with the provision that left-sided (dominant hemisphere) forebrain structures appear to be predominantly involved in vagal regulation, whereas homotopic right (non-dominant) forebrain regions seem to primarily control sympathetic tone and responses [Guo CC et al, 2016; Winkelmann T, 2017]. However, the **lateralization** model of autonomic control of the heart remains **controversial** [Thayer JF et al, 2012; Yoo HJ et al, 2017; Carnevali L et al, 2018]. The variability found in these studies is probably because of individual patterns of connectivity between the DLPFC and other cortical and

subcortical structures. In a TMS/fMRIS, Vink JJT et al [2018] found that only 4 under 9 participants had the subgenual cingulate cortex activated by stimulation of the DLPFC. One single session of excitatory transcranial direct current stimulation (tDCS) over the left DLPFC reduced HR and favored a larger vagal prevalence prior to stress exposure, moderated stress-induced HR acceleration and sympathetic activation/vagal withdrawal [Carvenali L et al, 2020]. Similar results were found with bifrontal tDCS [Nikolin S et al, 2017] which raises again the question about the effect of laterality when stimulating the DLPFC with the aim to increase vagus nerve activity.

Montenegro RA et al [2011] assessed the effects of anodal tDCS over the T3 scalp position (aims to reach the insular cortex) on measures of cardiac autonomic control. The authors found that the parasympathetic activity (HF(log)) increased and the sympathetic activity (LF(log)) and sympatho-vagal balance (LF/HF(log)) decreased in athletes but not in untrained individuals. No significant changes in HRV indexes were provoked by sham stimulation in both groups. The authors attributed the specific results to neuroanatomical and functional changes in the brain induced by long-term exercise training. Furthermore, Piccirillo G et al [2016] demonstrated that anodal tDCS over T3 scalp position reduced sinus sympathetic activity and increased vagal sinus activity and baroreflex sensitivity in older, but not younger individuals.

Taking together, those studies suggest that stimulation of the left dorsolateral prefrontal or the insular cortex with rTMS or tDCS increase vagal activity [review: Baptista AF et al, 2020; Iseger TA, 2020].

We consider it appropriate to recall that back in 2013 in our laboratory were documented relationships between HRV and EEG parameters, and in part of the current sample [Popovych IL et al, 2013; 2014; Babelyuk VYe et al, 2017]. In agreement with the cited authors, we found unidirectional changes under the influence of bilirubin spectrum power of both HF band (generated by vagus nuclei) and dorsolateral prefrontal cortex nuclei, which are projected on F3/F4 loci, but only those that generate **theta** rhythm, instead the nerve nuclei located there, which generate **beta** rhythm, change its power in the opposite way. Differently directed from the HF band changes the power of the **beta** rhythm at the T4 locus and the **alpha** rhythm at the T3 locus, which suggests that their source (according to Romodanov AP [1993]) is sympathoexcitatory neurons of the right and left amygdala, respectively. Instead, the source of the **delta** rhythm in the T4 locus, given the sign of the factor load, is probably the right insular cortex. Naturally, the power of the LF band HRV as a marker of sympathetic tone, as well as LF/HF ratio change reciprocally.

However, this applies to other loci, so there is no reason to talk about any local (topical) effect of bilirubin on nerve structures.

It is time to find out the mechanism of the neurotropic action of bilirubin. Only three decades after the discovery of the aryl hydrocarbon receptor (AhR), bilirubin was added to its list of numerous agonists.

Phelan D et al [1998] thought so. Although no endogenous physiological ligand for the AhR has yet been described, persistent expression of hepatic CYP1A1 gene expression (an AhR-dependent response) in congenitally jaundiced Gunn rats indirectly supports the existence of such a ligand(s) in these animals. High plasma levels of the heme degradation product bilirubin in these animals prompted authors to evaluate whether bilirubin is an endogenous AhR agonist. Expression of dioxin responsive element (DRE)-driven luciferase gene expression in stably transfected mouse, guinea pig, rat, and human cells was induced by treatment with physiological concentrations of bilirubin. Biliverdin, the metabolic precursor of bilirubin, also induced luciferase activity in all species. Both chemicals not only stimulated AhR transformation and DRE binding in vitro and in cells in culture, but competitive inhibition of [³H]TCDD-specific binding to the cytosolic AhR revealed that these chemicals

are AhR ligands. The significantly greater inducing potency of these chemicals in intact cells, compared to their ligand binding and AhR transformation potency in vitro, suggests that bilirubin and biliverdin may also be converted within the cell to a more potent activator(s).

Recently, the AhR, an ancient protein that possesses highly conserved functions across various species, has been associated with **brain** aging and age-associated diseases [Eckers A et al, 2016; Ojo ES et al, 2021]. Apart from its well-described role in xenobiotic metabolism, AhR plays a critical role in the developing **nervous** system of invertebrates and vertebrates. Dioxin, a ubiquitous environmental pollutant, avidly binds to this receptor, and maternal exposure to dioxin has been shown to impair higher **brain** functions and **dendritic** morphogenesis, possibly via an AhR-dependent mechanism. Kimura E & Tohyama C [2017] analyzed AhR mRNA expression in the **brains** of embryonic, juvenile, and adult mice by reverse transcription (RT)-PCR and *in situ* hybridization. In early brain development (embryonic day 12,5), AhR transcript was detected in the innermost **cortical** layer. The mRNA was also expressed in the **hippocampus, cerebral cortex, cerebellum, olfactory bulb**, and rostral migratory stream on embryonic day 18,5, postnatal days 3, 7, and 14, and in 12-week-old (adult) mice. **Hippocampal** expression was abundant in the CA1 and CA3 pyramidal and dentate gyrus granule cell layers, where expression level of AhR mRNA in 12-week old is higher than that in 7-day old. These results reveal temporal and spatial patterns of AhR mRNA expression in the mouse brain, providing the information that may contribute to the elucidation of the **physiologic and toxicologic significance of AhR in the developing brain.**

In neuronal progenitor cells, AhR interacts with its partners to direct differentiation into several neuronal subtypes, as well as to influence **dendrite** morphogenesis [Latchney SE et al, 2013]. Although AhR expression decreases from the embryonic period into adult life [Kimura E & Tohyama C, 2017], several physiological functions remain in the **adult brain**, which include the **regulation of neurotransmitter levels,** blood-brain barrier functions, and immune responses [Wang X et al, 2011; Chen WC et al, 2019].

In HT22 **hippocampal** neuronal cells, the activation of AhR by α-naphthoflavone (α-NF) induces the phosphorylation of MAPK, leading to **cell death in an AhR-dependent manner**. Inhibition of AhR by an AhR antagonist reduced αNF-induced cell death. Finally, inhibition of MAPKs reduced αNF-induced transcriptional activity of AhR [Yu AR et al, 2019].

AhR activation in **glial** cells by the microbial metabolism of dietary tryptophan interferes with the NF-κB inflammatory transcription program, thereby reducing **neuroinflammation**, which raises the possibility that this pathway could be targeted in **neurodegenerative and autoimmune** diseases in the CNS [Rothhammer V et al, 2016; 2018]. In addition to several gut microbiota metabolites, 6-formylindolo [3,2-b] carbazole (FICZ), an **endogenous** ligand of AhR, promotes **neurogenesis in adult neurons**, which is needed for **hippocampal** memory maintenance in mice.

AhR activation can regulate several genes involved in multiple aspects of **synaptic plasticity and neurogenesis** after brain development.

The administration of classic **AhR** exogene **agonist** dioxin (TCDD) in the **adult** brain **upregulates** the genes required for **synaptic plasticity and neuronal activities**, including genes encoding for postsynaptic density 95 (PSD-95) protein and early growth response 1 (EGR1) [Chen Y et al, 2017]. The conditional deletion of AhR in adult mice also showed that AhR activation is necessary for **subgranular zone of the hippocampal dentate gyrus** (SGZ) neurogenesis by increasing the number of newborn granule cells in the dentate gyrus of the hippocampus, which in turn improves hippocampus-dependent memory [De la Parra J et al, 2018].

FICZ, an **endogenous ligand of AhR**, showed positive effects on the fate of neuronal stem/progenitor cells by **upregulating** the ASCL1 and Ngn2 genes necessary for neuronal differentiation in the SGZ area of the **adult** mouse **hippocampus** [Keshavarzi M et al, 2020]. Additionally, AhR activation by FICZ improves hippocampal-dependent memory and learning tasks, which [Grabert K et al, 2016] was reversed following treatment with the AhR antagonist, CH22319 [Keshavarzi M et al, 2020].

Taking into account AhR activation and knockout studies, the **normal physiological function of AhR in adult brain neurons is to enhance neurogenesis and synaptic plasticity**.

ACCORDANCE TO ETHICS STANDARDS

Tests in patients are carried out in accordance with positions of Helsinki Declaration 1975 and directive of National Committee on ethics of scientific researches. During realization of tests from all participants the informed consent is got and used all measures for providing of anonymity of participants.

REFERENCES

1. Shapiro SM, Conlee JW. Brainstem auditory evoked potentials correlate with morphological changes in Gunn rat pups. Hear Res. 1991;57:16-22.
2. Watchko JF, Kernicterus and the molecular mechanisms of bilirubin-induced CNS injury in newborns. Neuromolecular Med. 2006;8:513-529.
3. Dennery PA, Seidman DS, Stevenson DK. Neonatal hyperbilirubinemia. N Engl J Med. 2001;344:581-590.
4. Watchko JF, Tiribelli C. Bilirubin-induced neurologic damage - Mechanisms and management approaches. N Engl J Med. 2013;369:2021-2030.
5. Chang FY, Lee CC, Huang CC, Hsu KS. Unconjugated bilirubin exposure impairs hippocampal long-term synaptic plasticity. PLoS One. 2009;4(6):e5876. doi:10.1371/journal.pone.0005876
6. Dani C, Pratesi S, Ilari A, Lana D, Giovannini MG, Nosi D, Buonvicino D, Landucci E, Bani D, Mannaioni G, Gerace E.et al. Neurotoxicity of Unconjugated Bilirubin in Mature and Immature Rat Organotypic Hippocampal Slice Cultures. Neonatology. 2019;115(3):217-225. doi:10.1159/000494101
7. Dani C, Pratesi S, Mannaioni G, Gerace E. Neurotoxicity of Unconjugated Bilirubin in Neonatal Hypoxic-Ischemic Brain Injury in vitro. Front Pediatr. 2021;9:659477. doi:10.3389/fped.2021.659477
8. Liang M, Yin X-L, Shi H-B, Li C-Y, Li X-Y, Song N-Y, Shi H-S, Zhao Y, Wang L-Y, Yin S-K. Bilirubin augments Ca^{2+} load of developing bushy neurons by targeting specific subtype of voltage-gated calcium channels. Sci Rep. 2017;7:431.
9. Han G-Y, Li C-Y, Shi H-B, Wang J-P, Su K-M, Yin X-L, Yin S-K. Riluzole is a promising pharmacological inhibitor of bilirubin-induced excitotoxicity in the ventral cochlear nucleus. CNS Neurosci Ther. 2015;21:262-270.
10. Chai S, Li M, Lan J, Xiong Z-G, Saugstad JA, Simon R. P. A kinase-anchoring protein 150 and calcineurin are involved in regulation of acid-sensing ion channels ASIC1a and ASIC2a. J Biol Chem. 2007;282:22668-22677.
11. Allen NJ, Attwell D. Modulation of ASIC channels in rat cerebellar Purkinje neurons by ischaemia-related signals. J Physiol. 2002;543:521-529.
12. Lai K, Song X-L, Shi H-S, Qi X, Li Ch-Y, Fang J, Wang F, Maximyuk O, Krishtal O, et al. Bilirubin enhances the activity of ASIC channels to exacerbate neurotoxicity in neonatal hyperbilirubinemia in mice. Sci Transl Med. 2020;12(530):eaax1337.

13. Goryachkovskiy AM. Clinical Biochemistry. Odesa: Astroprint; 1998: 608. [in Russian].

14. Heart Rate Variability. Standards of Measurement, Physiological Interpretation, and Clinical Use. Task Force of ESC and NASPE. Circulation. 1996;93(5):1043-1065.

15. Berntson GG, Bigger JT jr, Eckberg DL, Grossman P, Kaufman PG, Malik M, Nagaraja HN, Porges SW, Saul JP, Stone PH, Van der Molen MW. Heart Rate Variability: Origines, methods, and interpretive caveats. Psychophysiology. 1997;34:623-648.

16. Baevskiy RM, Ivanov GG. Heart Rate Variability: theoretical aspects and possibilities of clinical application. Ultrazvukovaya i funktsionalnaya diagnostika. 2001;3:106-127. [in Russian].

17. Shaffer F, Ginsberg JP. An Overview of Heart Rate Variability Metrics and Norms. Front Public Health. 2017;5:258. doi:10.3389/fpubh.2017.00258

18. Kul'chyns'kyi AB, Kyjenko VM, Zukow W, Popovych IL. Causal neuro-immune relationships at patients with chronic pyelonephritis and cholecystitis. Correlations between parameters EEG, HRV and white blood cell count. Open Medicine. 2017;12(1):201-213.

19. Popadynets' O, Gozhenko A, Badyuk N, Popovych I, Skaliy A, Hagner-Derengowska M, Napierata M, Muszkieta R, Sokołowski D, Zukow W, Rybałko L. Interpersonal differences caused by adaptogen changes in entropies of EEG, HRV, immunocytogram, and leukocytogram. JPES. 2020;20(Suppl 2):982-999.

20. Gozhenko AI, Korda MM, Popadynets' OO, Popovych IL. Entropy, Harmony, Synchronization and their Neuro-endocrine-immune Correlates. Odesa. Feniks; 2021: 232. [in Ukrainian].

21. Buzsaki G. Theta oscillations in the hippocampus. Neuron. 2002;33:325–340.

22. Romodanov AP (editor). Postradiation Encephalopathy. Experimental Researches and Clinical Observations. Kyiv:USRI of Neurosurgery;1993:224. [in Ukrainian and Russian].

23. Benarroch EE. The central autonomic network: functional organization, dysfunction, and perspective. Mayo Clin Proc. 1993;68(10):988-1001. doi:10.1016/s0025-6196(12)62272-1

24. Palma JA, Benarroch EE. Neural control of the heart: recent concepts and clinical correlations. Neurology. 2014;83:261-271. doi: 10.1212/WNL.0000000000000605

25. Thayer JF, Lane RD. Claude Bernard and the heart-brain connection: further elaboration of a model of neurovisceral integration. Neurosci Biobehav Rev. 2009;33(2):81-88. doi:10.1016/j.neubiorev.2008.08.004

26. Verberne AJ. Medullary sympathoexcitatory neurons are inhibited by activation of the medial prefrontal cortex in the rat. Am J Physiol. 1996;270(4Pt2):R713-R719. doi:10.1152/ajpregu.1996.270.4.R713

27. Verberne AJ, Lam W, Owens NC, Sartor D. Supramedullary modulation of sympathetic vasomotor function. Clin Exp Pharmacol Physiol. 1997;24(9-10):748-754. doi:10.1111/j.1440-1681.1997.tb02126.x

28. Gianaros PJ. Brain-body pathways to cardiovascular disease risk. In: Herbert Weiner Early Career Award Lecture, 66th Annual Meeting of the American Psychosomatic Society, Baltimore, MD, March 2008.

29. Sakaki M, Yoo HJ, Nga L, Lee TH, Thayer JF, Mather M. Heart rate variability is associated with amygdala functional connectivity with MPFC across younger and older adults. Neuroimage. 2016;139:44-52. doi:10.1016/j.neuroimage.2016.05.076

30. Iseger TA, Padberg F, Kenemans JL, Gevirtz R, Arns M. Neuro-Cardiac-Guided TMS (NCG-TMS): Probing DLPFC-sgACC-vagus nerve connectivity using heart rate - First results. Brain Stimul. 2017;10(5):1006-1008. doi:10.1016/j.brs.2017.05.002

31. Remue J, Vanderhasselt MA, Baeken C, Rossi V, Tullo J, De Raedt R. The effect of a single HF-rTMS session over the left DLPFC on the physiological stress response as measured by heart rate variability. Neuropsychology. 2016;30(6):756-766. doi:10.1037/neu0000255

32. Guo, CC, Sturm V E, Zhou J, Gennatas ED, Trujillo AJ, Hua AY, et al. Dominant hemisphere lateralization of cortical parasympathetic control as revealed by frontotemporal dementia. Proc Natl Acad Sci USA. 2016;113:E2430–E2439. doi: 10.1073/pnas.1509184113

33. Winkelmann T, Thayer JF, Pohlack S, Nees F, Grimm O, Flor H. Structural brain correlates of heart rate variability in a healthy young adult population. Brain Struct Funct. 2017;222(2):1061-1068. doi:10.1007/s00429-016-1185-1

34. Thayer JF, Åhs F, Fredrikson M, Sollers JJ 3rd, Wager TD. A meta-analysis of heart rate variability and neuroimaging studies: implications for heart rate variability as a marker of stress and health. Neurosci Biobehav Rev. 2012;36(2):747-756. doi:10.1016/j.neubiorev.2011.11.009

35. Yoo HJ, Thayer JF, Greening S, Lee TH, Ponzio A, Min J, Sakaki M, Nga L, Mather M, Koenig J. Brain structural concomitants of resting state heart rate variability in the young and old: evidence from two independent samples. Brain Struct Funct. 2018;223(2):727-737. doi:10.1007/s00429-017-1519-7

36. Carnevali L, Koenig J, Sgoifo A, Ottaviani C. Autonomic and Brain Morphological Predictors of Stress Resilience. Front Neurosci. 2018;12:228.

37. Vink JJT, Mandija S, Petrov PI, van den Berg CAT, Sommer IEC, Neggers SFW. A novel concurrent TMS-fMRI method to reveal propagation patterns of prefrontal magnetic brain stimulation. Hum Brain Mapp. 2018;39(11):4580-4592. doi:10.1002/hbm.24307

38. Carnevali L, Pattini E, Sgoifo A, Ottaviani C. Effects of prefrontal transcranial direct current stimulation on autonomic and neuroendocrine responses to psychosocial stress in healthy humans. Stress. 2020;23(1):26-36. doi:10.1080/10253890.2019.1625884

39. Nikolin S, Boonstra TW, Loo CK, Martin D. Combined effect of prefrontal transcranial direct current stimulation and a working memory task on heart rate variability. PLoS One. 2017;12:e0181833.

40. Montenegro RA, Farinatti P de TV, Fontes EB, Soares PP da S, Cunha da FA, Gurgel JL et al. Transcranial direct current stimulation influences the cardiac autonomic nervous control. Neurosci Lett. 2011;497(1):32-36. doi:10.1016/j.neulet.2011.04.019

41. Piccirillo G, Ottaviani C, Fiorucci C, Petrocci N, Moscucci F, Di Iorio C et al. Transcranial direct current stimulation improves the QT variability index and autonomic cardiac control in healthy subjects older than 60 years. Clin Interv Aging. 2016;11:1687-1695. doi:10.2147/CIA.S116194

42. Baptista AF, Maciel ABR, Okano AH, Moreira A, Campos ACP, Fernandes AM, et al. Neuromodulation and inflammatory reflex: Perspectives on the use of non-invasive neuromodulation in the management of disorders related to COVID-19. Preprint. 2020. May: 31.

43. Iseger TA, van Bueren NER, Kenemans JL, Gevirtz R, Arns M. A frontal-vagal network theory for Major Depressive Disorder: Implications for optimizing neuromodulation techniques. Brain Stimul. 2020;13(1):1-9. doi:10.1016/j.brs.2019.10.006

44. Popovych IL, Lukovych YuS, Korolyshyn TA, Barylyak LG, Kovalska LB, Zukow W. Relationship between the parameters heart rate variability and background EEG activity in healthy men. Journal of Health Sciences. 2013;3(4):217-240.

45. Popovych IL, Kozyavkina OV, Kozyavkina NV, Korolyshyn TA, Lukovych YuS, Barylyak LG. Correlation between Indices of the Heart Rate Variability and Parameters of Ongoing EEG in Patients Suffering from Chronic Renal Pathology. Neurophysiology. 2014;46(2):139-148.

46. Babelyuk VYe, Dubkowa GI, Korolyshyn TA, Holubinka SM, Dobrovol's'kyi YG, Zukow W, Popovych IL. Operator of Kyokushin Karate via Kates increases synaptic efficacy in the rat Hippocampus, decreases C3-θ-rhythm SPD and HRV Vagal markers, increases

virtual Chakras Energy in the healthy humans as well as luminosity of distilled water in vitro. Preliminary communication. JPES. 2017;17(1):383-393.

47. Phelan D, Winter GM, Rogers WJ, Lam JC, Denison MS. Activation of the Ah receptor signal transduction pathway by bilirubin and biliverdin. Arch Biochem Biophys. 1998;357(1):155-163. doi:10.1006/abbi.1998.0814

48. Eckers A, Jakob S, Heiss C, Haarmann-Stemmann T, Goy C, Brinkmann V, Cortese-Krott MM, Sansone R, Esser C, Ale-Agha N, et al. The aryl hydrocarbon receptor promotes aging phenotypes across species. Sci Rep. 2016;6:19618. doi:10.1038/srep19618.

49. Ojo ES, Tischkau SA. The Role of AhR in the Hallmarks of Brain Aging: Friend and Foe. Cells. 2021;10(10):2729. doi:10.3390/cells10102729

50. Kimura E, Tohyama C. Embryonic and Postnatal Expression of Aryl Hydrocarbon Receptor mRNA in Mouse Brain. Front Neuroanat. 2017;11:4. doi:10.3389/fnana.2017.00004.

51. Latchney SE, Hein AM, O'Banion MK, DiCicco-Bloom E, Opanashuk LA. Deletion or activation of the aryl hydrocarbon receptor alters adult hippocampal neurogenesis and contextual fear memory. J Neurochem. 2013;125:430-445. doi:10.1111/jnc.12130.

52. Wang X, Hawkins BT, Miller DS. Aryl hydrocarbon receptor-mediated up-regulation of ATP-driven xenobiotic efflux transporters at the blood-brain barrier. FASEB J. 2011;25:644–652. doi:10.1096/fj.10-169227.

53. Chen WC, Chang LH, Huang SS, Huang YJ, Chih CL, Kuo HC, Lee YH, Lee IH. Aryl hydrocarbon receptor modulates stroke-induced astrogliosis and neurogenesis in the adult mouse brain. J Neuroinflamm. 2019;16:187. doi:10.1186/s12974-019-1572-7.

54. Yu AR, Jeong YJ, Hwang CY, Yoon KS, Choe W, Ha J, Kim SS, Pak YK, Yeo EJ, Kang I. Alpha-naphthoflavone induces apoptosis through endoplasmic reticulum stress via c-Src-, ROS-, MAPKs-, and arylhydrocarbon receptor-dependent pathways in HT22 hippocampal neuronal cells. Neurotoxicology. 2019;71:39–51. doi:10.1016/j.neuro.2018.11.011.

55. Rothhammer V, Mascanfroni ID, Bunse L, Takenaka MC, Kenison JE, Mayo L, Chao CC, Patel B, Yan R, Blain M, et al. Type I interferons and microbial metabolites of tryptophan modulate astrocyte activity and central nervous system inflammation via the aryl hydrocarbon receptor. Nat Med. 2016;22:586–597. doi:10.1038/nm.4106.

56. Rothhammer V, Borucki DM, Tjon EC, Takenaka MC, Chao CC, Ardura-Fabregat A, de Lima KA, Gutierrez-Vazquez C, Hewson P, Staszewski O, et al. Microglial control of astrocytes in response to microbial metabolites. Nature. 2018;557:724–728. doi:10.1038/s41586-018-0119-x.

57. Chen Y, Xu L, Xie HQH, Xu T, Fu H, Zhang S, Sha R, Xia Y, Zhao B. Identification of differentially expressed genes response to TCDD in rat brain after long-term low-dose exposure. J Environ Sci. 2017;62:92–99. doi:10.1016/j.jes.2017.07.010.

58. De la Parra J, Cuartero MI, Perez-Ruiz A, Garcia-Culebras A, Martin R, Sanchez-Prieto J, Garcia-Segura JM, Lizasoain I, Moro MA. AhR Deletion Promotes Aberrant Morphogenesis and Synaptic Activity of Adult-Generated Granule Neurons and Impairs Hippocampus-Dependent Memory. eNeuro. 2018;5 doi:10.1523/ENEURO.0370-17.2018.

59. Keshavarzi M, Khoshnoud MJ, Ghaffarian Bahraman A, Mohammadi-Bardbori A. An Endogenous Ligand of Aryl Hydrocarbon Receptor 6-Formylindolo[3,2-b]Carbazole (FICZ) Is a Signaling Molecule in Neurogenesis of Adult Hippocampal Neurons. J Mol Neurosci. 2020;70:806–817. doi:10.1007/s12031-020-01506-x.

60. Grabert K, Michoel T, Karavolos MH, Clohisey S, Baillie JK, Stevens MP, Freeman TC, Summers KM, McColl BW. Microglial brain region-dependent diversity and selective regional sensitivities to aging. Nat Neurosci. 2016;19:504–516. doi:10.1038/nn.4222.